Original Article
Cite This: Colloid & Nanoscience Journal 2(1) (2024) 238-253.
CNJ.araku.ac.ir

Sulfonic acid-decorated magnetic nanostructure: an efficient hybrid catalyst for green synthesis of 1-Amidoalkyl-2-naphtholes

Mohammad Ali Bodaghifard[*1,2], **Hanieh Allahbakhshi**[1]

Received: 2024-07-08
Revised: 2024-08-31
Accepted: 2024-09-01
DOI: **10.52547/CNJ.2.1.238**

[1] Department of Chemistry, Faculty of Science, Arak University, Arak 3848177584, Iran.

[1]Institute of Nanosciences and Nanotechnology, Arak University, Arak, Iran.

Abstract

The remarkable stability of magnetic core and -OH functional groups on the surface of silica-coated magnetite (Fe_3O_4@SiO_2) nanoparticles make them an excellent candidate for functionalization and catalytic applications. In this study, a surface-modified solid support was fabricated by immobilizing sulfonic acid groups on magnetic nanoparticles (Fe_3O_4@SiO_2@AE-SO_3H). The structure of prepared hybrid nanostructure was characterized by various analyses, including Fourier-transform infrared spectroscopy (FT-IR), X-ray powder diffraction (XRD), thermogravimetric analysis (TGA/DTG), vibrating sample magnetometr (VSM), the field emission scanning electron microscopy (FE-SEM), and the electron-dispersive X-ray spectroscopy (EDS). The catalytic activity of prepared hybrid nanomaterial was assessed in the synthesis of 1-amidoalkyl-2-naphthols, resulting in high yields of the desired products under environmentally friendly conditions. High yields, short reaction times, green solvent and conditions, easy workup procedure, reusability without a significant diminish in catalytic efficiency and simple separation of nanocatalyst by using an external magnet alongside the environmental compatibility and sustainability are some advantages of this method.

Keywords: Hybrid nanostructure, Magnetic nanoparticles, Heterogeneous catalysis, 1-amidoalkyl-2-naphthols.

1. Introduction

Multicomponent reactions (MCRs) are highly effective synthetic tools that enable the simultaneous integration of multiple reactants into a single reaction, resulting in the creation of intricate molecules in a remarkably efficient manner [1]. These reactions provide numerous benefits over conventional stepwise synthesis methods, such as reduced reaction times, simplified work-up procedures, enhanced efficiency, cost-effectiveness, superior selectivity, and minimal environmental impact compared to classical organic chemistry [2]. Multicomponent reactions (MCRs) are a valuable tool in chemical synthesis, as they streamline the process by eliminating the need for multiple reaction steps. This not only saves time and resources but also reduces the overall reaction time and minimizes the use of solvents and reagents. Additionally, MCRs offer access to a wide range of structurally diverse compounds with high molecular complexity. This makes them particularly beneficial in drug discovery and development, where the ability to explore diverse chemical space is essential for identifying new lead compounds [3, 4].

In recent years, the principles of green chemistry have underscored the significance of creating environmentally friendly reaction conditions to minimize pollution. A notable advancement in this realm is the adoption of solvent-free conditions or green solvents, like water, in organic reactions. This transition from harmful solvents has spurred substantial progress in organic synthesis, fostering more sustainable and eco-friendly practices within the field [5, 6]. 1-amidoalkyl-2-naphthol derivatives are of increasing interest due to their biological activities and further use in the preparation of other important bioactive molecules, such as aminoalkyl naphthols. The 1-amidoalkyl-2-naphthols possess diverse biological properties, such as antiviral, antibacterial, antifungal, antioxidant, and antiparasitic qualities [7-12]. 1-amidoalkyl-2-naphthols can be also converted to 1,3-oxazine derivatives by an amide hydrolysis reaction, which exhibit anti-depression and anti-bradycardia effects [13].

Corresponding Authors: Mohammad Ali Bodaghifard
m-bodaghifard@araku.ac.ir

Numerous methods have been reported for synthesizing these compounds. However, these methods suffer from various drawbacks, including lengthy reaction times, the need for large quantities of costly and non-recyclable catalysts, the use of volatile and harmful solvents that contradict green chemistry principles, reflux conditions, and challenges in separating the final products. Therefore, there is a need for the development of more efficient and environmentally friendly approaches that yield higher quantities of the desired compounds under milder reaction conditions. Magnetic nanoparticles (MNPs) possess a large surface area and can be effortlessly separated using an external magnetic field, eliminating the need for tedious separation procedures typically associated with small nanoparticles [14]. However, magnetic nanoparticles can easily aggregate into larger clusters because of their anisotropic dipolar attraction. In addition, they have other deficiencies such as leaching under acidic conditions and being susceptible to autoxidation and toxicity. Therefore, it is crucial to protect the surface of these nanoparticles in order to mitigate these undesirable characteristics. Among the various inorganic compounds, silicon dioxide (SiO_2) is a standout candidate for surface protection due to its exceptional chemical and thermal stability. What sets SiO_2 apart is its ability to be easily modified by a wide range of functional groups, which in turn increases the chemical and colloidal stability of these compounds [15, 16-22]. Besides, using magnetic nanoparticles as catalysts is associated with other advantages including easy synthesis and functionalization, low toxicity and low cost [16-19].

One of the primary benefits of grafting and immobilizing active functional groups onto inorganic supports is the significant enhancement of catalytic activity. This process involves attaching molecules onto these supports, which effectively increases the surface area available for catalysis. As a result, more active sites are created for the reaction to take place, ultimately leading to a higher level of catalytic activity. Moreover, this innovative approach also offers improved selectivity in catalytic reactions. By grafting molecules onto magnetic nanosized inorganic supports, the separation process is simplified. The magnetic properties of these supports allow for easy separation from reaction mixtures using external magnets. In our ongoing pursuit to enhance the efficiency of heterogeneous nanocatalysts and promote environmentally friendly organic reactions in order to obtain valuable heterocyclic compounds [23-26], an acidic catalyst known as a heterogeneous hybrid nanostructure [Fe_3O_4@SiO_2@AE-SO_3H] was developed and thoroughly analyzed. The catalytic potential of Fe_3O_4@SiO_2@AE-SO_3H was evaluated for the production of 1-amidoalkyl-2-naphthols (Scheme 2).

2. Experimental

2.1. Materials

All reagents were purchased from reputable chemical companies (Merck, Across, Fluka) and were used without further purification. Melting points were measured by using electrothermal digital apparatus and are uncorrected. Obtained products were identified with comparison of their melting points and spectral data reported in the literature. Thin-layer chromatography (TLC) was utilized to monitor the progress of organic reactions, using a n-hexane/ethyl acetate (3:1) eluent.

2.2. Preparation of hybrid nanostructure [Fe_3O_4@SiO_2@AE-SO_3H]

Magnetite nanoparticles were prepared by co-preparation method [30]. The silica shell was coated onto Fe_3O_4 nanoparticles via hydrolysis of TEOS in basic solution [27]. The (3-choloropropyl)trimethoxysilane (CPTMS) as a linker was attached to the surface of nanoparticles. The nucleophilic substitution with aminoethanol affords the Fe_3O_4@SiO_2@AE nanostructure. Subsequently, the hybrid nanomaterial [Fe_3O_4@SiO_2@AE-SO_3H] was synthesized by reacting -NH and -OH groups and Chlorosulfonic acid. The final nanomaterial was then isolated using a magnet, washed with ethanol, and dried in a vacuum oven at 80 °C.

2.3. Acidity of Fe_3O_4@SiO_2@AE-SO_3H

The concentration of sulfonic acid groups was determined through a quantitative estimation using back titration with HCl (0.01 N). 2 mL of KOH (0.01 N) was added to 0.02 g of the Fe_3O_4@SiO_2@AE-SO_3H nanoparticles, and the mixture was stirred for a duration of 30 minutes. Following this, the catalyst was magnetically separated and washed with deionized water. The excess amount of KOH was then titrated with HCl (0.01 N) in the presence of phenolphthalein as an indicator. To ensure accuracy, three separate titrations were performed and the average value

was calculated to determine the acid amount of Fe_3O_4@SiO_2@AE-SO_3H. The results showed that this nanostructure possessed an acid amount of 3.2 mmol g^{-1}.

2.4. General procedure for One-pot Synthesis of 1-amidoalkyl-2-naphthols

In a test tube, a mixture of aldehydes (1 mmol), β-naphthol (1 mmol), amides (1.2 mmol) and Fe_3O_4@SiO_2@AE-SO_3H (20 mg) as a catalyst heated and stirred under solvent free conditions at 80 °C for the appropriate time. After completion of the reaction as monitored by TLC, the precipitate was diluted with hot ethanol (10 ml) and the catalyst was separated by an external magnet. The reaction mixture was cooled to room temperature and then filtered to obtain the crude products. The products were further purified through re-crystallization using a mixture of ethanol and water in a 4:1 ratio.

2.5. Selected spectroscopic data

N-((4-chlorophenyl)(2-hydroxynaphthalen-1-yl)methyl)acetamide (**4a**): ^{1}H NMR (DMSO-d_6): δ = 10.11 (1H, s, NH), 8.66 (2H, d, *J*= 8.4 Hz, H_{Ar}), 7.94 (2H, d, *J*= 8.4 Hz, H_{Ar}), 7.22-7.65 (7H, m, H_{Ar}, OH), 6.75 (1H, s, CH), 2.30 (3H, s, CH_3) ppm.; ^{13}C NMR (DMSO-d_6): δ = 191.5, 148.3, 144.9, 131.3, 131.2, 131.1, 130.1, 129.7, 129.2, 129.1, 128.9, 128.86, 128.83, 128.7, 127.5, 125.1, 123.7, 118.1, 47.5, 36.2 ppm.; Anal. Calcd. For $C_{19}H_{16}ClNO_2$: C, 70.05; H, 4.95; N, 4.30; Cl, 10.88; Found: C, 70.48; H, 5.07; N, 4.23; Cl, 10.79.

N-((2-hydroxynaphthalen-1-yl)(phenyl)methyl)benzamide (**4h**): ^{1}H NMR (DMSO-d_6): δ = 10.17 (1H, s, NH), 8.82 (1H, d, *J*= 6 Hz, H_{Ar}), 8.25 (1H, d, *J*= 6.6 Hz, H_{Ar}), 6.76-7.84 (16H, m, H_{Ar}, CH, OH) ppm.; ^{13}C NMR (DMSO-d_6): δ = 165.5, 153.7, 153.3, 151.3, 135.0, 132.9, 131.6, 131.4, 129.4, 128.85, 128.80, 128.7, 127.6, 126.5, 123.6, 122.9, 119.2, 119.0, 116.4, 112.5, 112.0 ppm.; Anal. Calcd. For $C_{24}H_{19}NO_2$: C, 81.56; H, 5.42; N, 3.96; Found: C, 81.73; H, 5.53; N, 4.03.

1-((2-hydroxynaphthalen-1-yl)(phenyl)methyl)urea (**4k**): ^{1}H NMR (DMSO-d_6): δ = 10.14 (1H, s, NH), 8.69 (1H, d, *J*= 6.3 Hz, H_{Ar}), 7.46-8.04 (14H, m, H_{Ar}, NH_2, OH), 6.93 (1H, s, CH) ppm.; ^{13}C NMR (DMSO-d_6): δ = 196.3, 153.1, 148.4, 146.3, 131.2, 131.1, 130.1, 129.5, 129.1, 127.7, 125.2, 124.2, 123.6, 118.2, 116.6 ppm.; Anal. Calcd. For $C_{18}H_{16}N_2O_2$: C, 73.95; H, 5.52; N, 9.58; Found: C, 74.07; H, 5.63; N, 9.67.

2.6. Characterization

The FT-IR spectra were recorded by Unicom Galaxy Series. The ^{1}H, ^{13}CNMR spectra for obtained products were reported on Brucker DRX-300 spectrometer operating at 300 and 75 MHz respectively in DMSO-d_6 with TMS as an internal standard. The crystal structure was carried out on by Philips Xpert Xray powder diffraction (XRD) diffract meter (Cu-Kα radiation and λ= 0.15406) in range of Bragg angle 10-80 using 0.05° as the step length. The thermal stability of prepared catalyst was investigated by a thermogravimetric analyzer with model Mettler TA4000 System under an N_2 atmosphere at a heating rate of 10 °Cmin^{-1}. The surface morphology and elemental content of catalyst was investigated on a Hitachi S-4160. The Elemental chemical analysis [energy dispersive X-ray spectroscopy (EDS)] coupled with SEM was reported for characterization of chemical elements of the prepared hybrid nanomaterial.

3. Result and discussion

3.1. Preparation and characterization of the hybrid nanostructure

The magnetic hybrid nanoparticles were prepared sequentially as depicted in Scheme 2. Magnetite (Fe_3O_4) nanoparticles were easily prepared via the chemical co-precipitation of Fe^{2+} and Fe^{3+} ions in basic solution and a layer of silica was placed on the magnetite nanoparticles to prevent their aggregation and oxidation. Then, the (3-chloropropyl)trimethoxysilane (CPTMS) as a linker was grafted to the surface of Fe_3O_4@SiO_2 particles under nitrogen atmosphere to produce the Fe_3O_4@SiO_2@PrCl nanostructure. In the subsequent stage, the chloro groups were replaced by a nucleophilic attack of ethanolamine. Ultimately, the nanoparticles were decorated with acidic groups through reacting of –NH and –OH groups with Chlorosulfonic acid. The resulting precipitate was washed with ethanol and d ried in the vacuum oven to gain the final hybrid nanomaterial [Fe_3O_4@SiO_2@AE-SO_3H]. The prepared nanostructure was characterized by various techniques, including Fourier-transform infrared spectroscopy (FT-IR), X-ray powder

diffraction (XRD), thermogravimetric analysis (TGA/DTG), field emission scanning electron microscopy (FE-SEM), and energy dispersive X-ray spectroscopy (EDS).

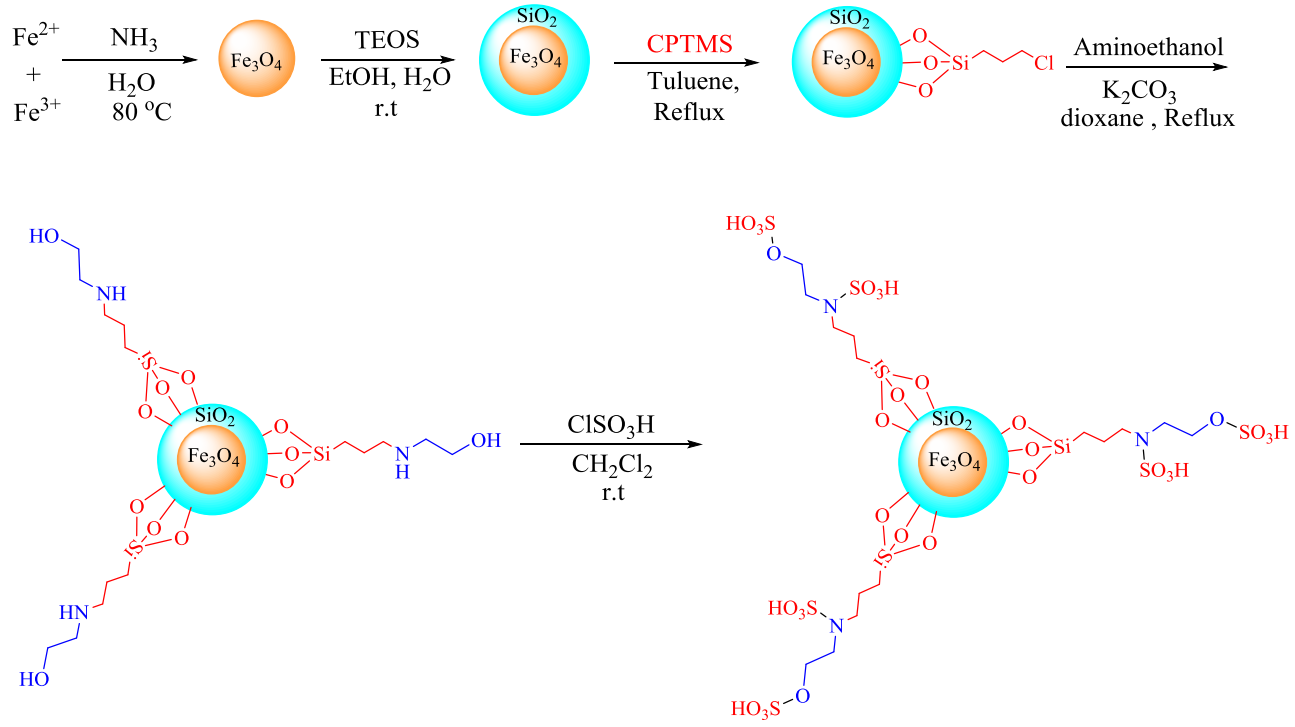

Scheme 1. Schematic steps for the construction of Fe_3O_4@SiO_2@AE-SO_3H hybrid nanostructure

3.2. FT-IR analysis

Fig. 1, shows the FT-IR spectra of Fe_3O_4, Fe_3O_4@SiO_2, Fe_3O_4@SiO_2-PrCl, Fe_3O_4@SiO_2-AE, Fe_3O_4@SiO_2@AE-SO_3H in the wavenumber range of 400–4000 cm^{-1}. The FT-IR spectrum of the bare magnetic Fe_3O_4 nanoparticles exhibited the characteristic Fe–O absorption band in the range of 580 cm^{-1} (Fig. 1a). The bands observed at 1101, 900–800, and 450 cm^{-1}, correspond to the asymmetric stretching, symmetric stretching, and in-plane bending of the Si–O-Si and Si–O bonds, respectively (Fe_3O_4@SiO_2 spectrum, Fig. 1b). The band in the region of 1300 cm^{-1} is related to the stretching bond S=O as depicted in Figure 1e. The broad band in the range of 3200–3500 cm^{-1} is attributed to the stretching vibration mode of Si–OH bonds, while the weak band at 1630 cm^{-1} related to the twisting vibration mode of H-O-H adsorbed in the silica layer. The existence of alkyl groups has been confirmed by the weak symmetric and asymmetric stretching vibrations at 2980 and 2895 cm^{-1} (Fig. 1c–e). Also, bands associated with C=N, C=C, and C-N were observed at 1350-1600 cm^{-1} (Fig. 1d–e) [27]. The N-H bending vibration overlaps with the O-H vibration. Consequently, these findings validate the effective bonding of various functional groups at each stage of fabrication.

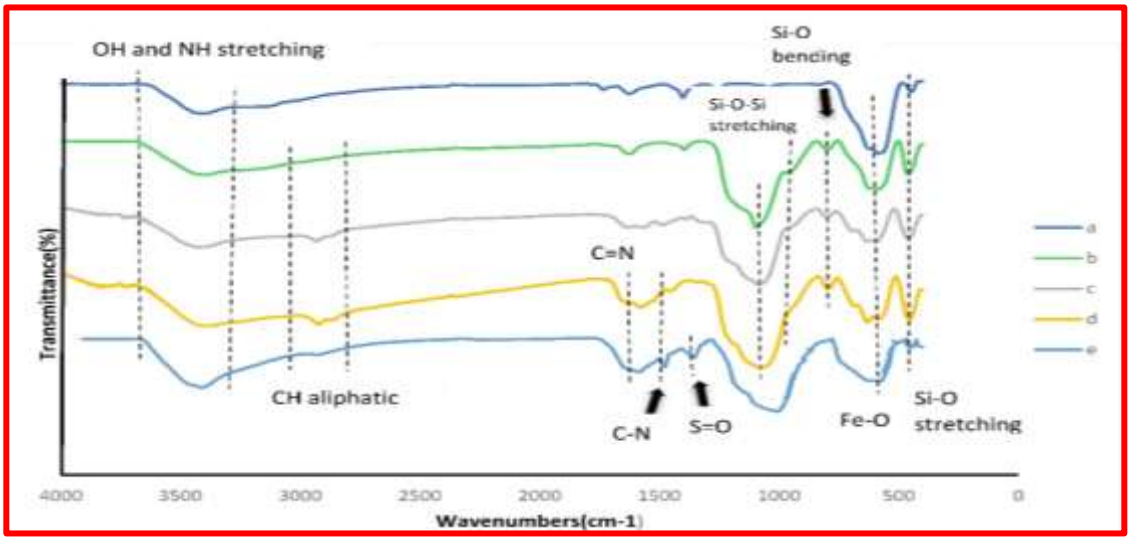

Fig. 1. FT-IR spectra of Fe_3O_4 (a), Fe_3O_4@SiO_2 (b), Fe_3O_4@SiO_2-PrCl (c), Fe_3O_4@SiO_2@AE (d), Fe_3O_4@SiO_2@AE-SO_3H (e).

3.3. XRD study

The crystallinity of Fe_3O_4 (a), and Fe_3O_4@SiO_2@EA-SO_3H (b) was analyzed using X-ray powder diffraction patterns (Fig. 2). Upon comparing the XRD patterns of Fe_3O_4 and Fe_3O_4@SiO_2@AE-SO_3H, it is evident that the ferrite core remains stable without undergoing any phase changes during the functionalization process. The XRD patterns of the prepared Fe_3O_4@SiO_2@AE-SO_3H material exhibit clear diffraction peaks at specific angles, including 2θ =30.2°, 35.4°, 43.7°, 56.6°, and 63.0°. These diffraction peaks correspond to the (220), (311), (400), (422), (511), and (440) Miller planes of Fe_3O_4 nanoparticles. XRD patterns confirm that the material structure possesses a cubic spinel phase as shown in Fig. 2a–b and align with the standard Fe_3O_4 sample (JCPDS file No. 19–0629) [28, 29]. The presence of the SiO_2 layer is confirmed by the appearance of a broad peak at 2θ = 18° to 25° (Fig. 2b). To determine the average crystallite size of Fe_3O_4@SiO_2@AE-SO_3H, the Scherrer equation ($D= K\lambda/\beta cos\theta$) was employed. In this equation, λ is the x-ray Cu wavelength, β is the width of the x-ray peak on the 2θ axis which measured as the line broadening at half the maximum intensity, θ is Bragg angle, and K is the so-called Scherrer constant. The crystallite size calculated from the width of the peak at 2θ= 35.4° (311), is approximately 33 nm [30].

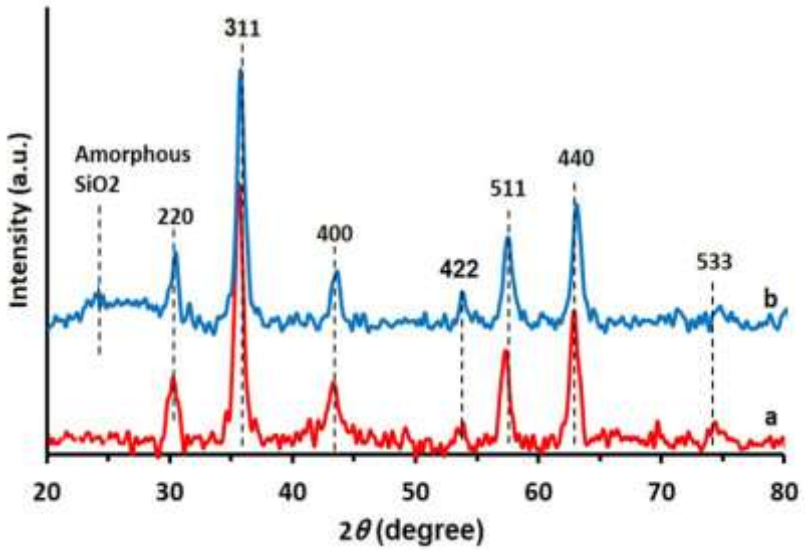

Fig. 2. XRD patterns of Fe_3O_4 (a), and Fe_3O_4@SiO_2@AE-SO_3H (b).

3.4. FE-SEM

The size and morphology of Fe_3O_4@SiO_2@AE-SO_3H were examined using field emission scanning electron microscopy (FE-SEM). The nanostructure of Fe_3O_4@SiO_2@AE-SO_3H displayed a nearly spherical shape, as depicted in Fig. 3, with an average size ranging from 20 to 50 nm.

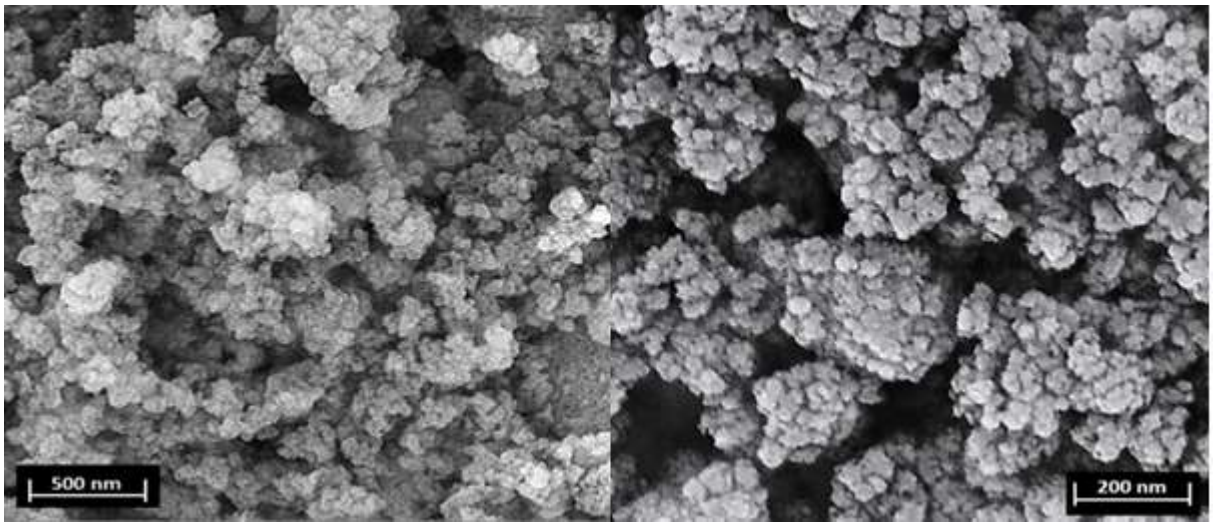

Fig. 3. The FE-SEM image of F_3O_4@SiO_2@AE-SO_3H

3.5. EDX analysis

The results obtained from X-ray energy diffraction spectroscopy (EDX) of Fe_3O_4@SiO_2@AE-SO_3H magnetic nanoparticles confirm the presence of elements S, C, N, Si, O, Fe in the hybrid nanostructure (Fig. 4). The higher intensity of the peak corresponding to the element Si and S elements compared to the Fe peak indicates that the Fe_3O_4 nanoparticles have been coated by SiO_2 layer and -SO_3H functionalities on the surface of the nanostructure. The terminal ends of the catalyst have a lot of -SO_3H groups, leading to a higher peak intensity for sulfur. These results provide strong evidence for the successful synthesis of the core-shell nanostructure (Fe_3O_4@SiO_2@AE-SO_3H).

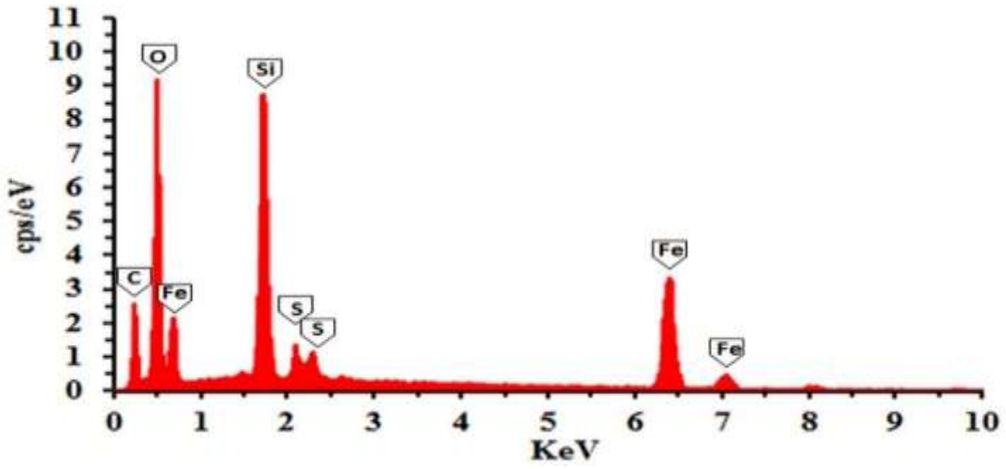

Fig. 4. EDX analysis for Fe_3O_4@SiO_2@AE-SO_3H

3.6. TGA

The thermogravimetric analysis (TGA) and derivative thermogravimetry (DTG) were used to determine the stability of the hybrid nanomaterial (Fig. 5). The magnetic catalyst (Fe_3O_4@SiO_2@AE-SO_3H) exhibits four distinct weight loss steps over the temperature range analyzed by TGA. The first step, including a low amount of weight loss at T < 250 °C, is due to the removal of physically adsorbed solvent and surface hydroxyl groups. the second stage at about 250 to nearly 650 °C is ascribed to the decomposition of the coating organic moiety in the nanocomposite. Thus, the weight loss between 250 and 600 °C gives the organic grafting ratios of the magnetic catalyst.

The observed weight loss at 600 °C temperatures and higher is related to the silica and nanoparticle groups, which is related to the phase change step. The slope of the curve represents good thermal resistance shown by the sample. Therefore, it can be concluded that almost the surface of the sample has been functionalized by organic groups. Analysis of the DTG chart reveals that decomposition of the organic structure primarily occurs between 300-600 °C, while the catalyst remains stable at temperatures up to 250 °C.

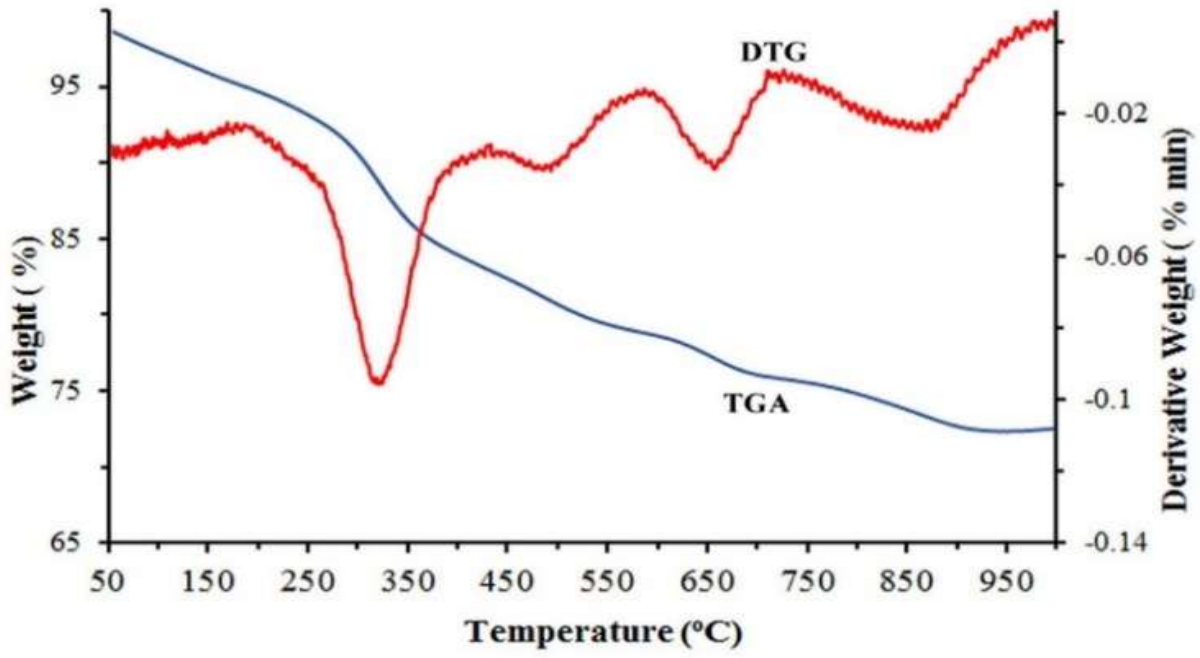

Fig. 5. TGA/DTG thermogram of Fe_3O_4@SiO_2@AE-SO_3H

3.7. VSM

The magnetic properties of the nanoparticles were characterized using a vibrating sample magnetometer (VSM). Figure 6 shows the plots of room temperature magnetization (*M*) versus magnetic field (*H*) (*M-H* curves or hysteresis loops) of Fe_3O_4 nanoparticles and Fe_3O_4@SiO_2@AE-SO_3H nanostructure. The hysteresis curve allows determination of the saturation magnetization (M_s), remanent magnetization (M_r) and coercivity (H_c). The magnetization of samples could be completely saturated at high fields of up to ±8000.0 Oe and the M_s of samples changed from 62 to 38 emu g^{-1}, due to the formation of a silica shell around the Fe_3O_4 core. The strong magnetization of the nanoparticles was also revealed by simple attraction with an external magnet (Fig. 6).

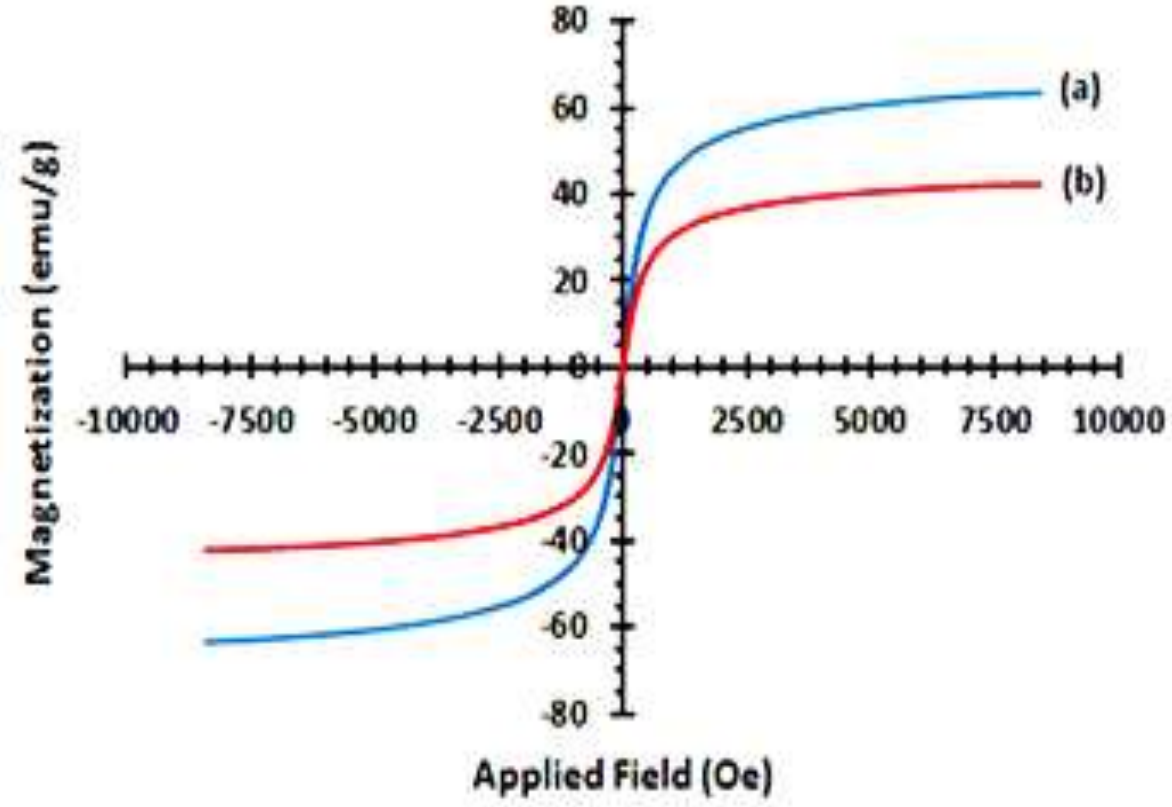

Fig 6. The magnetic hysteresis loops of Fe_3O_4 MNPs (a), and Fe_3O_4@SiO_2@AE-SO_3H (b)

3.8. Synthesis of 1-amidoalkyl-2-naphthols

After the successful preparation and characterization of Fe_3O_4@SiO_2@AE-SO_3H, its catalytic activity was considered in the synthesis of 1-amidoalkyl-2-naphthol derivatives. The reaction of 4-chlorobenzaldehyde (1 mmol), β-naphthol (1 mmol) and acetamide (1 mmol) was selected as a model reaction (Scheme 3), and parameters affecting the reaction yields such as temperature, solvent, catalyst amount, and the solvent-free conditions were investigated. Using the Fe_3O_4@SiO_2@AE-SO_3H as a catalyst, conventional heating at 90 °C under solvent-free conditions is the efficient and best condition. It was found that this reaction did not proceed significantly without catalyst and heating, even in a long time.

With the optimized conditions in hand, different amides and substituted aldehydes were reacted with β-naphthol in the presence of Fe_3O_4@SiO_2@AE-SO_3H (20 mg) via the one-pot multicomponent reaction to obtain substituted amidoalkyl naphthol derivatives. The results were summarized in Table 1. These reactions were very efficient and the desired products (4a-l) obtained in good to excellent yields (90-95%) in relatively short reaction times, without byproducts. Arylaldehydes with electron-donating or electron-withdrawing groups could lead to favorite products with no reasonable difference in their reactivity. The structure of 1-amidoalkyl naphthols was confirmed by FT-IR, 1H-NMR, ^{13}C-NMR spectroscopies and comparison with those reported in the literature. The catalytic activity of Fe_3O_4@SiO_2@AE-SO_3H MNPs for the model reaction was also compared with other reported catalysts, as shown in Table 3. The comparison of the Fe_3O_4@SiO_2@AE-SO_3H nanostructure as catalyst with some previously reported catalysts for the synthesis of 1-amidoalkyl-2-naphthol derivatives, confirm that the Fe_3O_4@SiO_2@AE-SO_3H is a comparable, suitable and efficient catalyst for synthesis of the desired corresponding products.

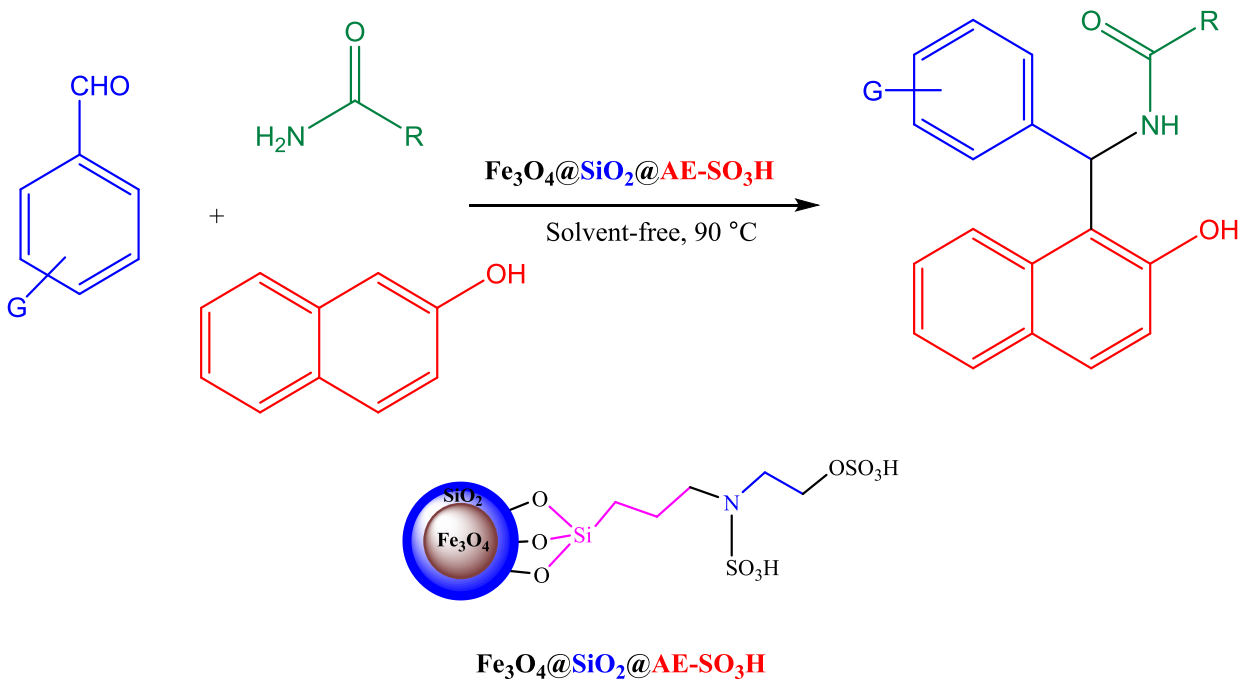

Scheme 2. Synthesis of 1-amidoalkyl-2-naphthol derivatives in the presence of Fe_3O_4@SiO_2@AE-SO_3H hybrid nanocatalyst

Table 1. Optimization of the reaction conditions for synthesis of 1-amidoalkyl-2-naphtoles [a]

Entry	catalyst (mg)	Solvent	Temperature (°C)	Time (min)	Yield (%)
1	Fe_3O_4@SiO_2@AE-SO_3H (10)	EtOH	70	80	78
2	Fe_3O_4@SiO_2@AE-SO_3H (10)	DMF	Reflux	60	41
3	Fe_3O_4@SiO_2@AE-SO_3H (10)	CH_3CN	Reflux	60	53
4	Fe_3O_4@SiO_2@AE-SO_3H (10)	Solvent-free	100	20	89
5	Fe_3O_4@SiO_2@AE-SO_3H (20)	Solvent-free	100	20	94
6	Fe_3O_4@SiO_2@AE-SO_3H (20)	Solvent-free	90	20	95
7	Fe_3O_4@SiO_2@AE-SO_3H (20)	Solvent-free	80	20	87
8	Fe_3O_4 (20)	Solvent-free	90	90	47
9	Fe_3O_4@SiO_2 (20)	Solvent-free	90	90	35
10	Fe_3O_4@SiO_2@AE (20)	Solvent-free	90	90	51
11	-	Solvent-free	90	240	15

[a] 4-chlorobenzaldehyde, 2-naphthol, Acetamide, catalyst.

Table 2. Synthesis of 1-amidoalkyl-2-naphtoles using Fe_3O_4@SiO_2@AE-SO_3H as a catalyst

Entry	ArCHO	Product	Time (min)	Yield[a] (%)	M.p. °C	
					Found	Reported
1	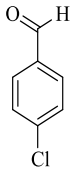	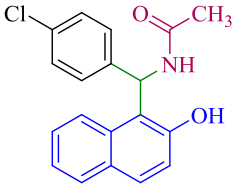 **(4a)**	20	95	225-227	220-222 [31]
2	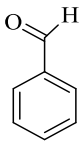	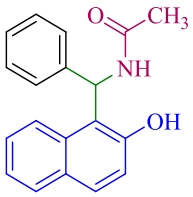 **(4b)**	20	91	238-241	239-240 [32]
3	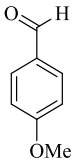	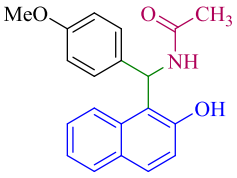 **(4c)**	25	90	182-184	183-185 [33]
4	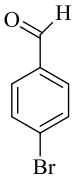	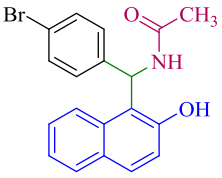 **(4d)**	15	95	223-225	226-227 [31]
5	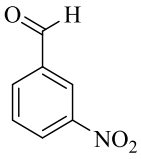	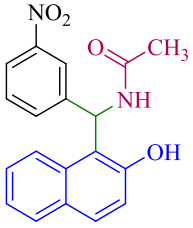 **(4e)**	20	94	252-254	254-255 [34]
6	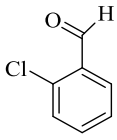	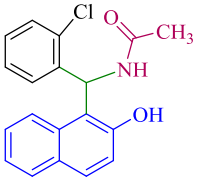 **(4f)**	20	90	203-205	205-206 [34]

7	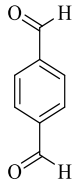	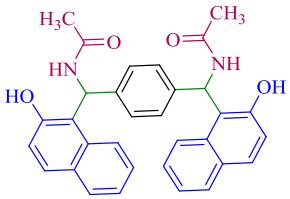 (4g)	25	92	275-277	277-279 [35]
8	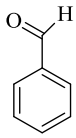	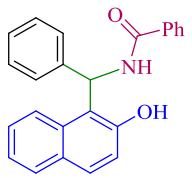 (4h)	20	93	230-232	232-234 [34]
9	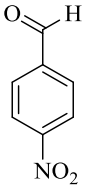	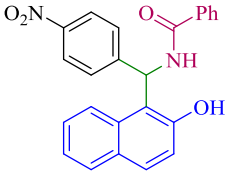 (4i)	15	95	238-241	238-240 [36]
10	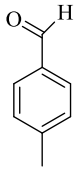	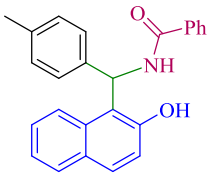 (4j)	20	93	204-205	200-202 [36]
11	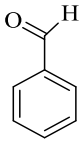	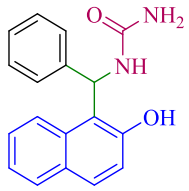 (4k)	15	93	174-177	173-175 [34]
12	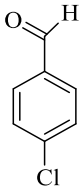	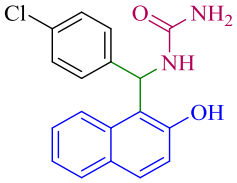 (4l)	20	91	172-174	168-170 [34]

[a] Isolated yield.

[b] The melting points are not corrected.

Table 3. The comparison of Fe_3O_4@SiO_2@AE-SO_3H as a catalyst with some other reported catalysts in the synthesis of 1-amidoalkyl-2-naphtoles

Entry	catalyst	condition	Time (min)	Yield (%)
1	Polyphosphate ester	Solvent-free, 80 °C	15	91 [34]
2	Trityl chloride	Solvent-free, 70 °C	15	94 [35]
3	[Dsim]HSO_4	Solvent-free, 80 °C	20	95 [32]
4	MNPs-PhSO_3H	Solvent-free, 120 °C	40	94 [31]
5	PTA/Mont. KSF Clay	Solvent-free, 125 °C	10	91 [36]
6	Zinc benzenesulfonate	Solvent-free, 80 °C	360	51 [37]
7	CdS-Fe_3O_4	CH_3CN, Reflux	60	93 [38]
8	Fe_3O_4@SiO_2@AE-SO_3H	Solvent-free, 90 °C	20	95 [This work]

The recovery and reusability of the catalyst are crucial for commercial and industrial applications, as well as for environmentally friendly processes. To investigate this, a study was conducted on the recovery and reusability of Fe_3O_4@SiO_2@AE-SO_3H in a model reaction involving 4-chlorobenzaldehyde, 2-naphthol, and acetamide (Fig. 7). After the reaction was completed, the resulting solidified mixture was diluted with 15 mL of hot EtOH. The catalyst was then easily separated, washed with hot EtOH, dried under vacuum, and reused in subsequent reaction. Impressively, nearly complete recovery of the catalyst (up to 97%) was achieved after each run. As shown in Figure 7a-b, the recycled catalyst maintained its effectiveness and stability even after being reused five times without any additional treatment or significant decrease in catalytic activity.

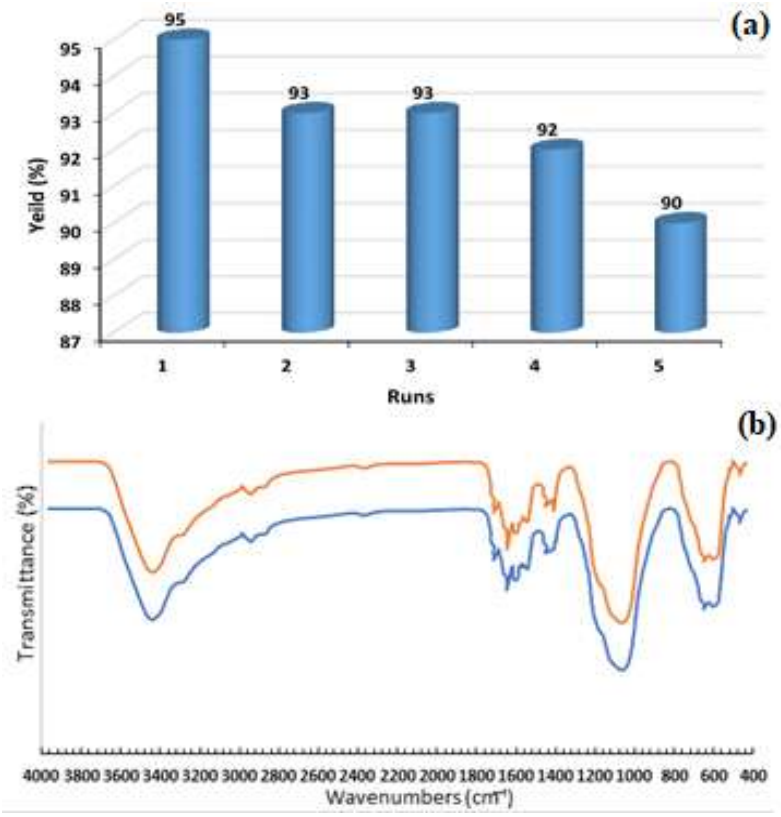

Fig. 7. (**a**) The recyclability of hybrid nanocatalyst (Fe_3O_4@SiO_2@AE-SO_3H) in the model reaction during five runs. (**b**) FT-IR spectra of the fresh and reused nanocatalyst

A plausible mechanism for the synthesis of 1-amidoalkyl-2-naphthols in the presence of $Fe_3O_4@SiO_2@AE\text{-}SO_3H$ is depicted in Scheme 3. The carbonyl group of the aldehyde is initially protonated by the acidic catalyst. Subsequently, 2-naphthole is enolized in acidic condition and undergoes condensation with activated aldehyde, leading to the formation of an intermediate (**I**). In the next step, the intermediate (**I**) is subjected to nucleophilic attack by deprotonated amide resulting in the production of final product. So, it is proposed that the H^+ ions act as Bronsted acids and activate the carbonyl functional groups and facilitate the condensation reactions. The porosity and high surface area of nanostructure ($Fe_3O_4@SiO_2@AE\text{-}SO_3H$) providing suitable support for the chemical reactions and increase the catalytic performance of the prepared hybrid nanomaterial.

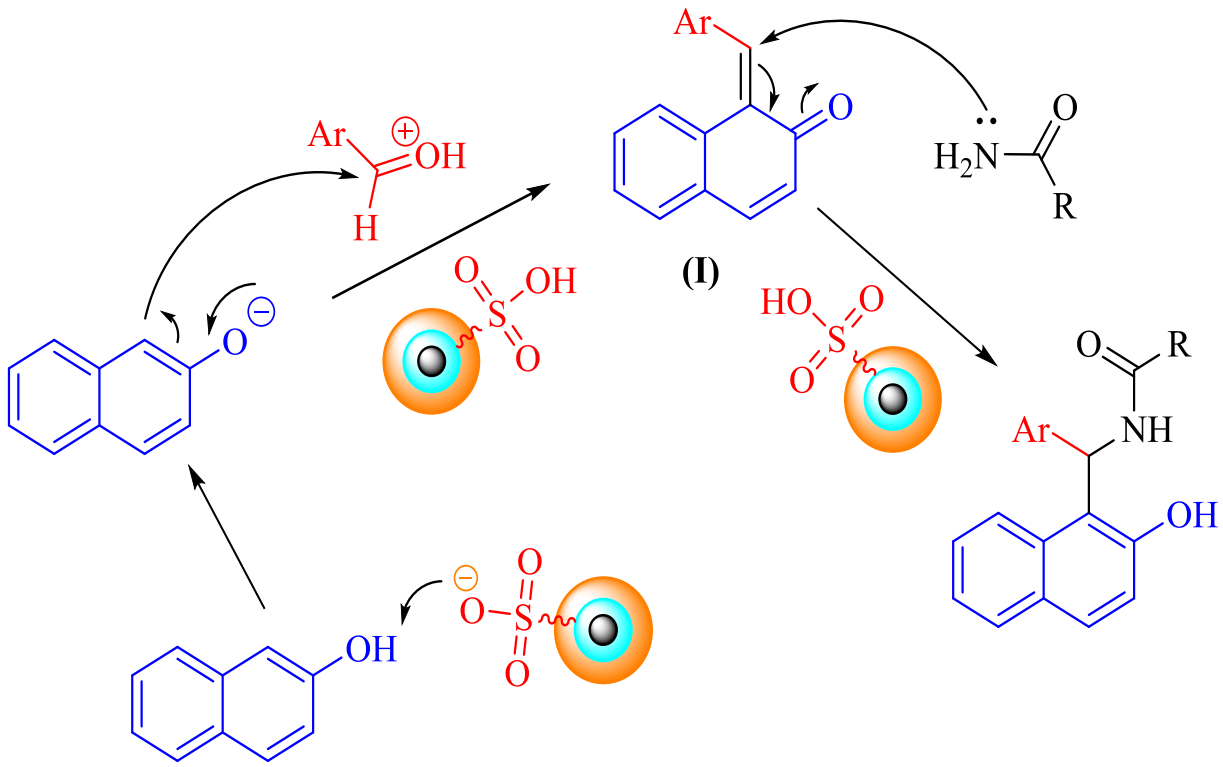

Scheme 3. The proposed path for synthesis of 1-amidoalkyl-2-naphthols using $Fe_3O_4@SiO_2@AE\text{-}SO_3H$ as a nanocatalyst

4. Conclusion

In this research, a novel heterogeneous solid acid catalyst has been successfully developed and characterized. The catalyst was synthesized by attaching aminoethanole moieties to silica-coated magnetic nanoparticles and then immobilizing sulfonic acid groups on its structure (known as $Fe_3O_4@SiO_2@AE\text{-}SO_3H$). The catalytic performance of this newly developed catalyst was evaluated in the synthesis of 1-amidoalkyl-2-naphthol derivatives. The desired products were obtained in high yields (90-95%) and short reaction times through a three-component reaction involving 2-naphthol, amides, and aldehydes. The comparison of the $Fe_3O_4@SiO_2@AE\text{-}SO_3H$ nanostructure as catalyst with some previously reported catalysts, confirm that the $Fe_3O_4@SiO_2@AE\text{-}SO_3H$ is a suitable and efficient catalyst for the synthesis of desired 1-amidoalkyl-2-naphthols. This approach offers numerous advantages, including high product yield and purity, a straightforward work-up process, environmental friendliness, minimal pollution, and easy catalyst separation. Furthermore, this hybrid nanocatalyst can be reused multiple times with only a slight decrease in its activity. Moreover, this heterogeneous solid acid catalyst shows promise for use in various chemical reactions.

Conflicts of Interest

The authors declare that they have no known competing financial interests or personal relationships that could have appeared to influence the work reported in this paper.

Author information

*Corresponding Author: Mohammad Ali Bodaghifard
m-bodaghifard@araku.ac.ir

ORCID

Mohammad Ali Bodaghifard: 0000-0001-9732-4746

Acknowledgements

The authors acknowledge the financial support of the Research Council of Arak University.

References

[1] J. Zhu, Q. Wang, M.-X. Wang, Multicomponent Reactions in Organic Synthesis. 1nd Edition, Wiley-VCH, Weinheim, Germany, 2015.

[2] J. Montgomery, Nickel-catalyzed cyclizations, couplings, and cycloadditions involving three reactive components. Acc. Chem. Res., 33 (2000) 467-473. https://doi.org/10.1021/ar990095d.

[3] R.V. Orru, M. de Greef, Recent advances in solution-phase multicomponent methodology for the synthesis of heterocyclic compounds. Synthesis, 2003 (2003) 1471-1499. http://dx.doi.org/10.1055/s-2003-40507

[4] L.F. Tietze, A. Modi, Multicomponent domino reactions for the synthesis of biologically active natural products and drugs. Med. Res. Rev., 20 (2000) 304-322. https://doi.org/10.1002/1098-1128(200007)20:4<304::AID-MED3>3.0.CO;2-8.

[5] R.C. Cioc, E. Ruijter, R.V. Orru, Multicomponent reactions: advanced tools for sustainable organic synthesis. Green Chem., 16 (2014) 2958-2975. https://doi.org/10.1039/C4GC00013G.

[6] A.K. Gupta, M. Gupta, Synthesis and surface engineering of iron oxide nanoparticles for biomedical applications. Biomaterials, 18 (2005) 3995-4021. https://doi.org/10.1016/j.biomaterials.2004.10.012.

[7] W.S.I. Abou-Elmagd, A.I. Hashem, Synthesis of 1-amidoalkyl-2-naphthols and oxazine derivatives with study of their antibacterial and antiviral activities. Med. Chem. Res., 22 (2013) 2005-2013. https://doi.org/10.1007/s00044-012-0205-9.

[8] B. Bananezhad, M.R. Islami, H. Khabazzadeh, Synthesis of novel amidoalkyl naphthol-based azo dyes and evaluation of their antimicrobial activities. J. Iran. Chem. Soc., 16 (2019) 865–877.

[9] M.A. Manavi, M.H.F. Nasab, F. Dashti, S. Moghimi, P. Saniee, B. Pouramiri, A. Foroumadi, M. Pirali-Hamedani, Green and one-pot synthesis of novel amidoalkyl naphthols using triethanolammonium acetate [$(OHCH_2CH_2)_3NH$][OAc]) ionic liquid and their anti-H.pylori activity. Res. Chem. Intermed. 48 (2022) 4049–4062.

[10] K. Boudebbous, N. Hamdouni, H. Boulebd, W. Zemamouche, A. Boudjada, A. Debache, Free radical scavenging activity and mechanisms of amidoalkyl-2-naphthol derivative: A joint experimental and theoretical study. Chem. Pap. 75 (2021) 6651–6660.

[11] N.R. Rode, A.A. Tantray, A.V. Shelar, R.H. Patil, S.S. Terdale, Synthesis, anti-leishmanial screening, molecular docking, and ADME study of 1-amidoalkyl 2-naphthol derivatives catalyzed by amino acid ionic liquid. Res. Chem. Intermed. 48 (2022) 2391–2412.

[12] K. Boudebbous, H. Boulebd, C. Bensouici, D. Harakat, R. Boulcina, A. Debache, Synthesis, Docking Study and Biological Activities Evaluation of 1-Amidoalkyl-2-naphthol Derivatives as Dual Inhibitors of Cholinesterase and α-Glucosidase. Chemistryselect 5 (2020) 5515-5520.

[13] H. Petkov, S.P. Simeonov, Amidoalkyl naphthols as important bioactive substances and building blocks: a review on the current catalytic Mannich-type synthetic approaches. Appl. Sci. 13 (2023) 6616. https://doi.org/10.3390/app13116616.

[14] W. Injumpa, P. Ritprajak, N. Insin, Size-dependent cytotoxicity and inflammatory responses of PEGylated silica-iron oxide nanocomposite size series. *J. Magn. Magn. Mater.*, 427 (**2017**) 60-66. https://doi.org/10.1016/j.jmmm.2016.11.015.

[15] S.H. Araghi, M.H. Entezari, Amino-functionalized silica magnetite nanoparticles for the simultaneous removal of pollutants from aqueous solution. *Appl. Surf. Sci.*, **2015**, *333*, 68-77. https://doi.org/10.1016/j.apsusc.2015.01.211.
[16] M.A. Bodaghifard, M. Hamidinasab, N. Ahadi, Recent advances in the preparation and application of organic-inorganic hybrid magnetic nanocatalysts on multicomponent reactions. Curr. Org. Chem. 22 (2018) 234-267. https://doi.org/ 10.2174/1385272821666170705144854.
[17] M.B. Gawande, P.S. Branco, R.S. Varma, Nano-magnetite (Fe_3O_4) as a support for recyclable catalysts in the development of sustainable methodologies. Chem. Soc. Rev. 42 (2013) 3371-3393. https://doi.org/10.1039/C3CS35480F.
[18] Zh.-H. Zhang, H.-Y. Lü, Sh.-H. Yang, J.-W. Gao. Synthesis of 2,3-dihydroquinazolin-4(1H)-ones by three-Component coupling of isatoic anhydride, amines, and aldehydes catalyzed by Magnetic Fe_3O_4 nanoparticles in water. J. Comb. Chem. 12 (2010) 643-646. https://doi.org/10.1021/cc100047j.
[19] Z. Mahhouti, H. El Moussaoui, T. Mahfoud, M. Hamedoun, M. El Marssi, A. Lahmar, A. El Kenz, A. Benyoussef, Chemical synthesis and magnetic properties of monodisperse cobalt ferrite nanoparticles. J. Mater. Sci. Mater. Electron., 30 (2019) 14913-14922. https://doi.org/10.1007/s10854-019-01863-3.
[20] S. Shylesh, V. Schünemann, W.R. Thiel, Magnetically separable nanocatalysts: bridges between homogeneous and heterogeneous catalysis. Angew. Chem. Int. Ed. 49 (2010) 3428-3459. https://doi.org/10.1002/anie.200905684.
[21] Y. Leng, K. Sato, Y. Shi, J. G. Li, T. Ishigaki, T. Yoshida, H. Kamiya, Oxidation-resistant silica coating on gas-phase-reduced iron nanoparticles and influence on magnetic properties. J. Phys. Chem. C 113 (2009) 16681-16685. https://doi.org/10.1021/jp902655r.
[22] A.L. Morel, S.I. Nikitenko, K. Gionnet, A. Wattiaux, J. Lai-Kee-Him, C. Labrugere, B. Chevalier, G. Deleris, C. Petibois, A. Brisson, M. Simonoff, Sonochemical approach to the synthesis of Fe_3O_4@SiO_2 core-shell nanoparticles with tunable properties. *ACS Nano*, **2008**, 2, 847.
[23] M.A. Bodaghifard, A. Mobinikhaledi, M. Hamidinasab, An efficient one-pot synthesis of 2, 3-dihydroquinazolin-4 (1H)-ones in green media. Synth. React. Inorg. Metal-Org. Nano-Met. Chem., 44 (2014), 567-571. https://doi.org/10.1080/15533174.2013.776605.
[24] M.A. Bodaghifard, Z. Faraki, A.R. Karimi, Mild synthesis of mono-, bis-and tris 1, 2-dihydrobenzo [4, 5] imidazo [1, 2-a] pyrimidine derivatives using alkyl disulfamic acid functionalized magnetic nanoparticles. Curr. Org. Chem., 20 (2016) 1648-1654.
[25] M.A. Bodaghifard, Palladium-melamine complex anchored on magnetic nanoparticles: A novel promoter for C-C cross coupling reaction. J. Organomet. Chem., 886 (2019) 57-64. https://doi.org/10.1016/j.jorganchem.2019.02.010.
[26] A. Mobinikhaledi, S. Asadbegi, M.A. Bodaghifard, Convenient, multicomponent, one-pot synthesis of highly substituted pyridines under solvent-free conditions. Synth. Commun., 46 (2016) 1605-1611. https://doi.org/10.1080/00397911.2016.1218516.
[27] M.A. Bodaghifard, S. Shafi, Ionic liquid-immobilized hybrid nanomaterial: an efficient catalyst in the synthesis of benzimidazoles and benzothiazoles via anomeric-based oxidation. J. Iran. Chem. Soc., 18 (2021) 677-687. https://doi.org/10.1007/s13738-020-02055-1.
[28] Q. Zhou, Y. Wu, Y. Sun, Xu. Sheng, Y. Tong, J. Guo, B. Zhou, J. Zhao, Magnetic polyamidoamine dendrimers for magnetic separation and sensitive determination of organochlorine pesticides from water samples by high performance liquid chromatography. J. Envron. Sci., 102 (2021) 64-73. https://doi.org/10.1016/j.jes.2020.09.005.
[29] S. Asadbegi, M.A. Bodaghifard, E. Alimohammadi, R. Ahangarani-Farahani, Immobilization of palladium on modified nanoparticles and its catalytic properties on Mizoroki-Heck reaction. ChemistrySelect, 3 (2018) 13297-13302. https://doi.org/10.1002/slct.201802501.
[30] V. Uvarov, I. Popov, Metrological characterization of X-ray diffraction methods for determination of crystallite size in nano-scale materials. Mater. Charact., 58 (2007) 883-891. https://doi.org/10.1016/j.matchar.2006.09.002.
[31] H. Moghanian, A. Mobinikhaledi, A.G. Blackman, E. Sarough-Farahani, Sulfanilic acid-functionalized silica-coated magnetite nanoparticles as an efficient, reusable and magnetically separable catalyst for the solvent-free synthesis of 1-amido- and 1-aminoalkyl-2-naphthols. RSC Adv., 4 (2014) 28176-28185. Doi: https://doi.org/10.1039/C4RA03676J.

[32] A. Zare, T. Yousofi, A.R. Moosavi-Zare, Ionic liquid 1,3-disulfonic acid imidazolium hydrogen sulfate: a novel and highly efficient catalyst for the preparation of 1-carbamatoalkyl-2-naphthols and 1-amidoalkyl-2-naphthols. RSC Adv., 2 (2012) 7988-7991. Doi: 10.1039/C2RA20679J.
[33] A. Khazaei, M. Zolfigol, A.R. Moosavi-Zare, A. Zare, A. Parhami, A. Khalafi-Nezhad, Trityl chloride as an efficient organic catalyst for the synthesis of 1-amidoalkyl-2-naphtols in neutral media at room temperature. Appl. Catal. A Gen., 386 (2010) 179-187. https://doi.org/10.1016/j.apcata.2010.07.057.
[34] H. Moghanian, S. Ebrahimi, Three component, one-pot synthesis of amidoalkyl naphthols using polyphosphate ester under solvent-free conditions. J. Saudi Chem. Soc., 18 (2014) 165-168. https://doi.org/10.1016/j.jscs.2011.06.017.
[35] A. Khazaei, M.A. Zolfigol, A.R. Moosavi-Zare, F. Abi, A. Zare, H. Kaveh, V. Khakyzadeh, M. Kazem-Rostami, A. Parhami, H. Torabi-Monfared, Discovery of an in situ carbocationic system using trityl chloride as a homogeneous organocatalyst for the solvent-free condensation of β-naphthol with aldehydes and amides/thioamides/alkyl carbamates in neutral media. Tetrahedron, 69 (2013) 212-218. https://doi.org/10.1016/j.tet.2012.10.042.
[36] D.P. Narayanan, R.M. Ramakrishnan, S. Sugunan, B.N. Narayanan, Solvent free one pot synthesis of amidoalkyl naphthols over phosphotungstic acid encapsulated montmorillonite clay catalysts. J. Saudi Chem. Soc., 21 (2017) 538-544. https://doi.org/10.1016/j.jscs.2015.10.007.
[37] M. Wang, Z.G. Song, Y. Liang, Zinc benzenesulfonate-promoted eco-friendly and efficient synthesis of 1-amidoalkyl-2-naphthols. Synth. Commun., 42 (2012) 582-588. https://doi.org/10.1080/00397911.2010.527424.
[38] C. Sun, Sh. Mao, D. Yu, M. Xue, X. Sun, Synthesis, characterization, and photocatalytic application of cadmium(II) sulfide-magnetite in one-pot multi-component synthesis of some 1-amidoalkyl-2-naphthols. J. Mol. Struct., 1312 (2024) 138451. https://doi.org/10.1016/j.molstruc.2024.1384